# Recombination of radical pairs in high magnetic fields: A path integral–Monte Carlo treatment

Klaus Schulten and Irving R. Epstein[a)]

*Max-Planck-Institut für biophysikalische Chemie, 3400 Göttingen-Nikolausberg, Federal Republic of Germany*

(Received 30 August 1978; accepted 27 March 1979)

The magnetic field dependence of photoinduced geminate hydrogen (electron) transfer processes originates from a Brownian motion of radical pairs, a hyperfine coupling, and Zeeman-induced precession of the unpaired electron spins and a spin-selective recombination. In this paper we introduce a Wiener path integral description for these processes. This approach entails an integration over all possible diffusion trajectories of two functionals, one that weights the diffusion paths according to the laws of Brownian motion, and a second that accounts for the spin motion and recombination of the radical pairs. This formulation maintains a close connection with the actual physical processes and is suitable for microscopic radical reaction processes under quite general circumstances. For the path integration we employ a Monte Carlo method, and for the electron spin precession we adopt a semiclassical approximation. The theory is then applied to the magnetic field dependence of a photoinduced hydrogen transfer process involving a ketyl–hexyl radical pair recently observed with nanosecond time resolution at fields of a few kG. It is argued that the magnetic field dependence observed cannot be reconciled with a simple hyperfine-coupled Zeeman-induced spin motion. Finally, a simple analytical expression for the magnetic field dependence of geminate radical pair recombination at high magnetic fields is presented.

## I. INTRODUCTION

Photochemical hydrogen abstraction involving geminate radical pair processes has played an important[1] albeit somewhat controversial[2,3] role in the understanding of the effect of chemically induced dynamic polarization of electron and nuclear spins. Theoretical descriptions based on the radical pair and triplet mechanisms have only provided a qualitative explanation of the observed NMR and ESR spectra. However, for a detailed understanding of radical pair processes, comparisons with such spectra, which are hampered by a poor time resolution as far as the geminate processes are concerned, can hardly be satisfactory. In this respect spectroscopic observations with a time resolution in the nanosecond range provide much needed information (cf. Ref. 4–6). Such measurements have been carried out recently by Staerk and Razi Naqvi[7] on hydrogen abstraction processes and, in this paper, we will provide a corresponding theoretical description. The theory applied is well developed in principle. We will carry out our calculations, however, in a novel way applying the Wiener path integral method,[8] which seems to be eminently suitable for the description of microscopic solvent processes. Our analysis is based on a recent semiclassical solution of the dynamics of the electron–nuclear spin motion.[9]

Photoinduced electron and hydrogen transfer processes produce in a *ps* to *ns* time range radical pairs, which either form geminate recombination products by backtransfer within a few nanoseconds or separate into long-lived ($\mu$s) radicals. The geminate process involves the diffusion of the radicals within the so-called solvent cage. The geminate recombination depends on the spin multiplicity of the radical pair, which determines if triplet (if energetically accessible) or singlet products are generated. It had been demonstrated that the spin multiplicity is governed by a coherent precession of the two unpaired electron spins of the radical pair (e.g., Ref. 4–6), the precession resulting from the hyperfine interaction between electron and neighboring nuclear spins as well as the Zeeman interaction with any applied magnetic field. The precession starts from a pure quantum (singlet or triplet) state, then alters the relative orientation of the electron spin pair thereby determining the spin multiplicity of the geminate recombination products. A variation of the applied magnetic field modulates the spin precession and, hence, the yield of recombination products.

Recently, Staerk and Razi Naqvi[7] observed a magnetic field effect on the recombination of the photogenerated ketyl–hexyl radical pair as presented in Fig. 1. Benzophenone in its triplet state ($^3B^*$) populated by an *ns* laser

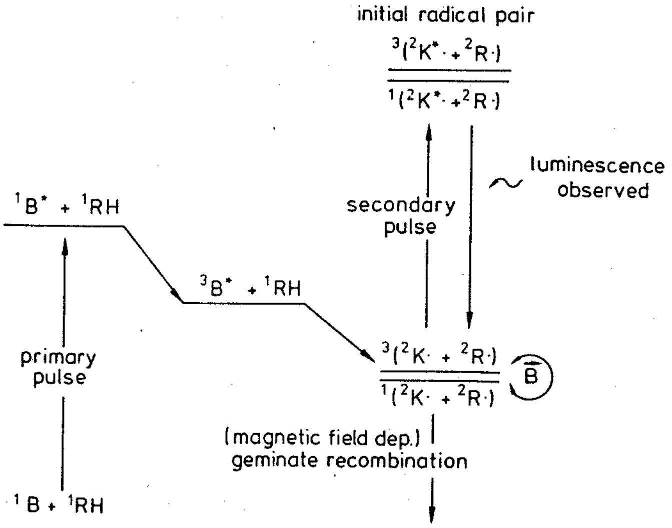

FIG. 1. Energy and reaction scheme for the photoinduced hydrogen abstraction processes involving the ketyl radical (see text).

---

[a)] Permanent address: Department of Chemistry, Brandeis University, Waltham, Mass. 02154.

0021-9606/79/010309-08$01.00

pulse at time $t=0$ abstracts hydrogen from the hexane solvent ($^1$RH) to generate a ketyl–hexyl radical pair $^2\mathrm{K}\cdot + {}^2\mathrm{R}\cdot$ in the triplet state

$$^3\mathrm{B}^* + {}^1\mathrm{RH} \rightarrow {}^3({}^2\mathrm{K}\cdot + {}^2\mathrm{R}\cdot) \ .$$

In the course of the subsequent spin precession the radical pair assumes partial singlet character

$$^3({}^2\mathrm{K}\cdot + {}^2\mathrm{R}\cdot) \rightarrow {}^1({}^2\mathrm{K}\cdot + {}^2\mathrm{R}\cdot) \ .$$

The generation of the pair is also followed by a Brownian motion leading to the separation of the pair after repeated reencounters, which for a time of a few nanoseconds, give the system a chance for hydrogen back transfer to the singlet ground state $^1\mathrm{B} + {}^1\mathrm{RH}$. The latter can occur only if the radical pair has adopted a singlet alignment of its unpaired electron spins. An external magnetic field alters the amount of singlet spin character of the pairs. As a result, the repopulation of $^1\mathrm{B} + {}^1\mathrm{RH}$ will be changed and, complementarily, also the concentration of ketyl radicals $^2\mathrm{K}\cdot$ at a time after geminate reencounters cease, i.e., at about $t \geq 10$ ns. At later times homogeneous recombination, which is independent of the applied field, will deplete the radicals. Staerk and Razi Naqvi monitored with a secondary laser pulse the concentration of $^2\mathrm{K}\cdot$ at time $t=38$ ns, i.e., at a time after the geminate re-encounters have taken place but before homogeneous recombination becomes important. These authors found that a field of 6 kG reduces the zero field concentration of $^2\mathrm{K}\cdot$ by about 8%, and they explained their observation by the spin mechanism outlined.

The generation, diffusion, spin motion, and recombination of a radical pair is described by coupled diffusion equations each representing the concentration of pairs in the different electron-nuclear spin states.[10] In Ref. 5 and 6 we employed a solution procedure, which in practice is rather limited, e.g., to spherically symmetric situations in the absence of exchange interaction. Here we will adopt instead the well-known path integral approach to diffusion processes, which traces for a sufficiently large number (~2000) of radical pairs the diffusion trajectories generated by a Monte Carlo procedure. This approach mimics the actual histories of the recombining radical pairs and can be generalized readily to anisotropic situations including exchange interactions.

In Sec. II we describe the spin precession of the ketyl–hexyl radical pair. It is argued already at this point that the observed magnetic field dependence of the recombination process cannot be reconciled with a hyperfine coupling and Zeeman interaction-induced electron spin motion. In Sec. III we introduce the path integral formulation of diffusion processes combined with a coherent spin motion and spin-selective reactions. In Sec. IV we calculate the magnetic field dependent yield of the ketyl–hexyl geminate recombination . Finally, in Sec. V, we present a model for which the high field geminate recombination yield is given by a simple analytical expression.

## II. SPIN MOTION

The unpaired electron spins in the ketyl and hexyl radicals carry out a coherent motion which is induced by the hyperfine interaction between electron and nuclear spins, by the Zeeman interaction with an external magnetic field B and, in case the radicals come into contact, by an exchange interaction. The spin Hamiltonian governing this motion is

$$H = H_1 + H_2 + J(\mathrm{r})\left(\tfrac{1}{2} + \mathrm{S}_1 \cdot \mathrm{S}_2\right) \ , \tag{1}$$

$$H_i = \left(g_i \mu \mathrm{B}/\hbar + \sum_k a_{ik} \mathrm{I}_{ik}\right) \cdot \mathrm{S}_i \ , \tag{2}$$

where $H_i$ $(i=1,2)$ contains the intramolecular Zeeman and hyperfine interactions ($g_i$ is the $g$ value, $a_{ik}$ are the hyperfine coupling constants, and $\mathrm{I}_{ik}$ the nuclear spins of radical $i$) and $J(\mathrm{r})$ represents the strength of the intermolecular exchange interaction. $H$ neglects the smaller nuclear Zeeman terms as well as all anisotropic contributions to hyperfine coupling and $g$ values. $J(\mathrm{r})$ rapidly decreases to zero with increasing radical separation $r$. The intramolecular spin interactions are only of order $10^{-4}$ eV and, upon approach of the radicals, $J(\mathrm{r})$ far exceeds $H_1 + H_2$. This results in a freezing of the spin motion in the contact region of the radicals. As the radicals reside in this narrow region of a few Å width only for very short times, the exchange interaction can be neglected for most of the life span. In this Section we will assume therefore $J(\mathrm{r})=0$. The influence of a nonvanishing exchange interaction will be considered in Secs. III and IV.

The hyperfine coupling constants of the ketyl radical are[11]:

$$\begin{aligned} 4\times a_H &= 2.52\ \mathrm{G}\ , \\ 4\times a_H &= 0.82\ \mathrm{G}\ , \\ 2\times a_H &= 3.50\ \mathrm{G}\ . \end{aligned} \tag{3}$$

In lieu of hexyl coupling constants we assumed the coupling constants of its butyl relative. It is not evident, however, if hydrogen abstraction by $^3B^*$ leads to the hexyl, sec-hexyl or tert-hexyl radical or a mixture thereof. We opted quite arbitrarily for a sec-hexyl structure and assigned the sec-butyl coupling constants[12]:

$$\begin{aligned} 1\times a_H &= 21.8\ \mathrm{G}\ , \\ 3\times a_H &= 24.5\ \mathrm{G}\ , \\ 2\times a_H &= 27.9\ \mathrm{G}\ . \end{aligned} \tag{4}$$

We may note, however, that the hexyl radical probably exhibits somewhat weaker hyperfine coupling judged by the sum of all coupling constants amounting to 151 G for the sec-butyl radical and to 104 G for the 3-butenyl analog of butyl.[12]

The quantity which governs the ketyl-hexyl recombination $^1({}^2\mathrm{K}\cdot + {}^2\mathrm{R}\cdot) \rightarrow {}^1\mathrm{B} + {}^1\mathrm{RH}$ and, hence, the concentration of ketyl, is the probability $p_S(t)$ that the radical pair exists in the singlet state $^1({}^2\mathrm{K}\cdot + {}^2\mathrm{R}\cdot)$ at time $t$. In evaluating this probability for a ketyl-hexyl pair generated initially ($t=0$) in a triplet state $^3({}^2\mathrm{K}\cdot + {}^2\mathrm{R}\cdot)$, we employ the semiclassical approximation developed by Schulten and Wolynes.[9] The probability is

$$p_S(t) = \tfrac{1}{3}\langle \mathrm{tr}[Q_S(t)\, Q_T(0)]\rangle \ . \tag{5}$$

$Q_S$ and $Q_T$ are the projection operators on the subset of singlet and triplet states, respectively. The treatment

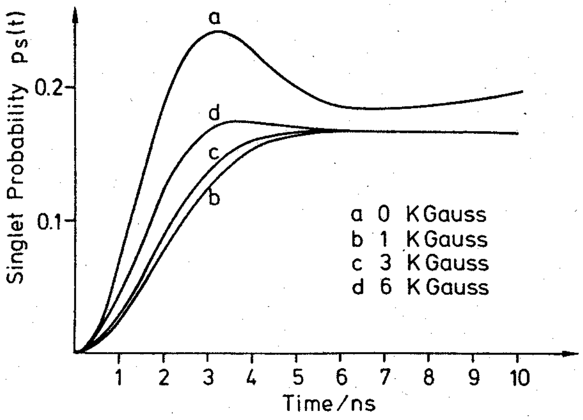

FIG. 2. Comparison of the singlet probabilities of a ketyl–hexyl radical pair starting ($t=0$) in the triplet state at different magnetic fields.

in Ref. 9 takes no account of a possible difference in the $g$ values of the radical pair which plays an important role in the high field behavior of the geminate recombination process. However, the corresponding modification of the the theory is a trivial matter and we will quote explicitly those expressions for $p_S(t)$ which deviate from the ones given in Ref. 9.

At zero field the Zeeman term in (2) vanishes and, hence, the expressions of Ref. 9 still apply, i.e.,

$$p_S(t)=\tfrac{1}{4}[1-g^{(0)}(t/\tau_1)g^{(0)}(t/\tau_2)]\,, \tag{6}$$

where

$$g^{(0)}(x)=\tfrac{1}{3}[1-2(1-2x^2)\exp(-x^2)]\,,$$

and[13]

$$\tau_i^{-2}=\frac{1}{6}\sum_k a_{ik}^2 I_{ik}(I_{ik}+1)\,. \tag{7}$$

At field strengths such that the Zeeman term $g_i\,\mu B/\hbar$ exceeds in magnitude the hyperfine term $\sum_k a_{ik}\mathbf{I}_{ik}$ the Hamiltonian $H$ couples only the states $S_0$ and $T_0$ leaving the nuclear spin configurations unaltered. This situation holds for field strengths much greater than $\sum_{i,k} a_{ik} \approx 171$ G, i.e., for fields above 1 kG. In the high field case the interaction responsible for the coupling of $S_0$ and $T_0$ is (the magnetic field B is taken parallel to the $z$ axis)

$$V=\tfrac{1}{2}\Big[(g_1-g_2)\mu B/\hbar+\sum_k a_{1k}M_{1k}-\sum_l a_{2l}M_{2l}\Big](S_{1z}-S_{2z})\,. \tag{8}$$

At short times the singlet probability at zero field exceeds its values at high field as long as the $\Delta g=g_1-g_2$ contribution to $V$ is negligible. However, since this contribution increases linearly with the field, sufficiently high fields will make $p_S(t)$ ultimately exceed its zero field values. For the evaluation of the high field singlet probabilities one needs to modify the expressions of Ref. 9 slightly:

$$p_S(t)=\tfrac{1}{6}[1-\cos(\Delta\omega t)\,e^{(0)}(t/\tau_1)\,e^{(0)}(t/\tau_2)]\,, \tag{9}$$

where

$$e^{(0)}(x)=\exp(-x^2)$$

and

$$\Delta\omega=(g_1-g_2)\,\mu B/\hbar\,. \tag{10}$$

The singlet probabilities evaluated by means of Eqs. (6)–(10) are presented in Fig. 2. Unfortunately, the $g$ values of the ketyl–hexyl pair are not known. We assumed a value $\Delta g=10^{-2}$ which probably represents the upper limit of the actual value.[14] The results in Fig. 2 demonstrate that the ketyl–hexyl pair develops about 20% singlet character soon after its generation. An external field of 1 kG reduces the singlet probability. A further increase of the field strength, however, induces an increase in the probability values. Yet, rather large fields above 10 kG are needed to exceed the zero field singlet probability at short times. This finding is at variance with the observations of Staerk and Razi Naqvi[7] who reported that fields of a few kG suffice to decrease the concentration of the ketyl radicals below the zero field value. For this to happen the $\Delta g$ contribution must be at least of the same magnitude as the average hyperfine contribution of (8), i.e.,

$$\Delta g\,B\approx\pi\Big[\frac{1}{2}\sum_{i,k}a_{ik}^2\Big]^{1/2}=138\text{ G}\,, \tag{11}$$

which corresponds ($\Delta g=0.01$) to $B\approx 14$ kG. A smaller $\Delta g$ value would raise this field even higher. For fields smaller than 14 kG to be effective the hyperfine coupling must be significantly weaker than 138 G.

The following remark regarding the contribution of the $\Delta g$ effect is of importance: the factor $\cos(\Delta\omega t)$ accounting for this effect in Eq. (9) is multiplied by $f_{NE}(t)=e^{(0)}(t/\tau_1)\,e^{(0)}(t/\tau_2)$. The factor $f_{NE}(t)$ decays to zero and, hence, attenuates the $\Delta g$ effect with time. The origin of this behavior is the spread of nuclear spin configurations in a random sample of radical pairs which entails a corresponding spread of spin precession frequencies, leading to a decay of "spin memory" of the sample as a whole.

## III. PATH INTEGRAL DESCRIPTION

The magnetic field modulated recombination of radical pairs entails a coherent spin motion and a Brownian motion and is described by a stochastic Liouville equation.[5,6,10] Under conditions which prevail in most cases the Liouville equation can be reduced to two coupled diffusion equations for the concentration of radical pairs in the singlet state $c_S(\mathbf{r},t)$ and in the triplet state $c_T(\mathbf{r},t)$, respectively.[5,6]

$$\frac{\partial}{\partial t}c_S(\mathbf{r},t)=[D\nabla^2-\kappa s(\mathbf{r})]c_S(\mathbf{r},t)+\dot{p}_S(t)\,[c_S(\mathbf{r},t)+c_T(\mathbf{r},t)]\,, \tag{12a}$$

$$\frac{\partial}{\partial t}c_T(\mathbf{r},t)=D\nabla^2c_T(\mathbf{r},t)-\dot{p}_S(t)\,[c_S(\mathbf{r},t)+c_T(\mathbf{r},t)]\,. \tag{12b}$$

$\mathbf{r}$ denotes the relative distance between the radicals, $t$ the time since generation, $D\nabla^2$ is the free diffusion operator where $D$ is the (relative) diffusion constant, $s(\mathbf{r})$ describes the domain in which hydrogen back-transfer takes place $[\int d\mathbf{r}\,s(\mathbf{r})=1]$, and $\kappa$ is the rate of this reaction. The solution of Eqs. (12a) and (12b) is subject to the initial condition

$$c_S(\mathbf{r}, t=0)=0\ , \tag{12c}$$

$$c_T(\mathbf{r}, t=0)=I(\mathbf{r})\ , \tag{12d}$$

fixing the spatial distribution $I(\mathbf{r})$ of the radical pairs in the triplet state at $t=0$. We will assume $\int d\mathbf{r}\, I(\mathbf{r})=1$, i.e., we want Eq. (12) to describe a single pair. $p_S(t)$ denotes the probability that the radical pair has adopted singlet character in case no reaction takes place, i.e., $\kappa=0$. In Ref. 6 we applied a solution procedure to Eq. (12) based on a finite difference approximation which, however, is limited to rather restricted physical situations. Here we want to adopt instead the path integral approach.

Path integration, introduced by Wiener, has been widely employed for the description of Brownian motion.[8] Applied to Eq. (12) the Wiener path integral,

$$c_{S,T}(\mathbf{r}, t/\mathbf{r}_0, t_0)=\int_{(\mathbf{r}_0,t_0)}^{(\mathbf{r},t)} q_{S,T}[\mathbf{r}(t)] \times \exp\left[-\frac{1}{4D}\int_{t_0}^{t} \dot{\mathbf{r}}(t')^2\, dt'\right] d[\mathbf{r}(t)]\ , \tag{13}$$

gives the probability for a radical pair starting the diffusion process at distance $\mathbf{r}_0$ at time $t_0$ in the triplet state to appear at distance $\mathbf{r}$ at time $t$ in the singlet $[c_S(\mathbf{r}, t/\mathbf{r}_0, t_0)]$ or in the triplet $[c_T(\mathbf{r}, t/\mathbf{r}_0, t_0)]$ state. The integration extends over all diffusion paths $\mathbf{r}(t)$ connecting $(\mathbf{r}_0, t_0)$, i.e., $\mathbf{r}(t_0)=\mathbf{r}_0$, and $(\mathbf{r}, t)$. The contribution of each path is weighted by the exponential functional

$$\exp\left[-\frac{1}{4D}\int_{t_0}^{t} \dot{\mathbf{r}}(t')^2\, dt'\right]\ . \tag{14}$$

The paths are characterized in addition by the functional $q_{S,T}[\mathbf{r}(t)]$ which accounts for the spin motion as well as the spin-selective recombination $^1(^2\mathrm{K}\cdot + {}^2\mathrm{R}\cdot) \rightarrow {}^1\mathrm{B} + {}^1\mathrm{RH}$ of the radical pair. $q_{S,T}$ is defined through the first order differential equations

$$\dot{q}_S[\mathbf{r}(t)]=\dot{p}_S(t)\{q_S[\mathbf{r}(t)]+q_T[\mathbf{r}(t)]\}-\kappa s[\mathbf{r}(t)]q_S[\mathbf{r}(t)]\ , \tag{15a}$$

$$\dot{q}_T[\mathbf{r}(t)]=-\dot{p}_S(t)\{q_S[\mathbf{r}(t)]+q_T[\mathbf{r}(t)]\}\ , \tag{15b}$$

subject to the initial condition

$$q_S[\mathbf{r}(0)]=0\ , \tag{15c}$$

$$q_T[\mathbf{r}(0)]=1\ , \tag{15d}$$

These equations bear an obvious interpretation.

The actual evaluation of the path integral (13) is carried out by a Monte Carlo technique.[15] The path $\mathbf{r}(t)$ is represented by pairs $(\mathbf{r}_0, t_0)$, $(\mathbf{r}_1, t_1)$, $(\mathbf{r}_2, t_2), \ldots, (\mathbf{r}_N, t_N) = (\mathbf{r}, t)$ and $\dot{\mathbf{r}}=(\mathbf{r}_i-\mathbf{r}_{i-1})/(t_i-t_{i-1})$ is assumed constant in the time intervals $[t_{i-1}, t_i]$. The weight (14) corresponding to this path is $\Pi_{i=1}^{N} \exp[-(\mathbf{r}_i-\mathbf{r}_{i-1})^2/4D(t_i-t_{i-1})]$. One chooses therefore the pairs $(\mathbf{r}_i, t_i)$ in a random fashion so as to conform to this weighting, i.e., one first selects $\Delta t_i = t_i - t_{i-1}$ and then chooses the distance $\mathbf{d}_i=\mathbf{r}_i-\mathbf{r}_{i-1}$ from the Gaussian distribution

$$[4\pi D\Delta t_i]^{-3/2}\exp[-\mathbf{d}_i^2/4D\Delta t_i]\ . \tag{16}$$

(In actuality we adopted a Monte Carlo procedure which takes advantage of the spherical symmetry imposed on the radical recombination process.) While propagating the reaction path the functionals $q_{S,T}[\mathbf{r}(t)]$ are being integrated. In effect this calculation procedure mimics the diffusion path of a radical pair and, therefore, maintains a close connection with the actual physical process of the magnetic field modulated recombination. In this respect this method is superior to a straightforward numerical integration procedure as has been adopted, for example, in Ref. 6. Also, the Monte Carlo technique is quite flexible and lends itself to the treatment of phenomena such as an exchange interaction, which would be exceedingly difficult to deal with otherwise. The major drawback of this technique is that large amounts of computer time are required to simulate enough pairs in order to reduce statistical uncertainties to an acceptable level.

In the following we present a brief account of the numerical procedures involved in our Monte Carlo approximation to the path integral (13). The calculation is begun by generating an ensemble of radical pairs at $t_0=0$, in a pure triplet state. Since the probability of recombination in any time interval $[t_i, t_{i-1}]$ is quite small it is appropriate to follow an ensemble or swarm of pairs, reducing its effective weight by the corresponding recombination probability at each step rather than to monitor an individual pair which either survives a trajectory step or recombines and disappears. Such an approach has proved successful in the calculation of positron annihilation spectra,[16] a process which bears a close analogy to the present problem.

The spins evolve deterministically according to Eq. (15) in a manner specified by the $\Delta g$ value of the radical pair, the external magnetic field and the size of the exchange region, if any. The triplet → singlet transition rates $\dot{p}_S(t)$ have been evaluated for $\Delta g=0.01$ and for fields 0, 1, 2, ..., 9 kG (i.e., corresponding to the singlet probabilities in Fig. 2), and are stored over a uniform time grid of spacing 0.33 ns. A standard calculation employed the same probabilities for all fields, i.e., one set of diffusion paths leads to recombination yields for all conditions.

The trajectories are obtained by the method of Ermak[15] for particles in a force-free environment. One radical is assumed to be fixed, while the other radical moves during each step with a constant velocity in a uniformly distributed random direction. The distance traveled in each step is chosen from the distribution (16). The stationary radical is assumed to be a hard sphere of radius $r_0=6$ Å. If the moving particle strikes the sphere, it is specularly reflected. This behavior at the boundary can be derived from the Green's function for free diffusion near a reflective wall. The time interval $\Delta t$ is chosen initially so that $\sqrt{2D\Delta t} \ll r_f - r_0$, where $r_f$ is the outer radius of the reaction region beyond which $s(\mathbf{r})$ vanishes. This condition assures an accurate description of the initial sharp diffusion distribution. For a reaction domain with $r_f - r_0 = 1$ Å an initial time increment $\Delta t$ of $10^{-4}$ ns is satisfactory. As the particle moves further from the sphere, the step size $\Delta t$ may be increased considerably, speeding up the calculation without any adverse effect on its accuracy. Generally we choose $\Delta t$ for a particle outside the reaction region such that were the particle to travel directly toward the center of the fixed reaction partner, it would just reach the reaction region. However, $\Delta t$ was not allowed to exceed the spacing between the grid points at which the spin transition rates $\dot{p}_S(t)$ were stored.

The actual recombination is described by a Feshbach optical potential $Q_S \kappa s(\mathbf{r})$ surrounding the stationary radical. ($Q_S$ here is the projection operator on the singlet radical pair states.) The potential has been assumed to be spherical and to have the form of a step function

$$s(\mathbf{r}) = \begin{cases} s_0 \text{ if } r_0 \leq r \leq r_f , \\ 0 \text{ if } r > r_f . \end{cases} \tag{17}$$

In the present application we have chosen $\kappa$ such that the reaction $^1(^2\mathrm{K}\cdot + {}^2\mathrm{R}\cdot) \rightarrow {}^1\mathrm{B} + {}^1\mathrm{RH}$ is "90% diffusion controlled," i.e.,[5] $[1 + D/\kappa r_0(r_f - r_0)]^{-1} = 0.9$.

For each step of the trajectory the fraction $f$ of $\Delta t$ spent by the particle inside the reaction region $r \leq r_f$ is calculated. The singlet recombination yield for that step is then given by

$$\delta_S = \bar{q}_S \left[1 - \exp(-\kappa s_0 f \Delta t)\right] , \tag{18}$$

where

$$\bar{q}_S = \tfrac{1}{2}\{q_S[\mathbf{r}(t)] + q_S[\mathbf{r}(t+\Delta t)]\} \tag{19}$$

is the average singlet population during the step neglecting recombination, i.e., updating the spin populations $q_S[\mathbf{r}(t)]$ and $q_T[\mathbf{r}(t)]$ using the transition probabilities $\dot{p}_S(t+\Delta t)$ and $-\dot{p}_S(t+\Delta t)$, respectively. The singlet population $q_S[\mathbf{r}(t+\Delta t)]$ is then reduced by the recombination yield $\delta_S$ before the next trajectory step begins. An ensemble is followed until some preset maximum time is reached, at which point a new ensemble is generated.

The program requires 18 K of storage on the Univac 1108. Each ensemble takes about 10 s of computer time to evaluate the yields of all field strengths when the maximum diffusion time is set at 9.5 ns and the optical potential extends from 6 to 7 Å. For an optical potential reaching only to 6.5 Å computation time is reduced by about 30% because particles are more likely to be beyond the reaction region where larger $\Delta t$'s can be employed.

In order to demonstrate the flexibility of the path integral approach, we have also undertaken calculations for radical recombination in the presence of a strong exchange interaction $J(\mathbf{r})$. When $J(\mathbf{r})$ greatly exceeds the intramolecular spin interactions $H_i$ the triplet → singlet transitions are suppressed and, since all pairs start in the nonreactive triplet state, the recombination yield is lowered. The exact form of $J(\mathbf{r})$ is not known. We choose to model the exchange effects by introducing an exchange region such that spin transitions are forbidden within the region and occur freely outside. In terms of the Monte Carlo approximation all that is required is a calculation of the time spent inside the exchange region for each trajectory step. The time argument of the spin probability $p_S(t)$ in Eq. (15) is then simply the laboratory time minus the time spent in the exchange region, i.e., the spin driving term $p_S(t)$ of Eq. (15) becomes a functional of the reaction path $\mathbf{r}(t)$.

In order to demonstrate the accuracy of the Monte Carlo approximation to the Wiener path integral we have carried out a corresponding calculation for the solution of the equation

$$\frac{\partial}{\partial t} d(\mathbf{r}, t) = [D\nabla^2 - \kappa s(\mathbf{r})] d(\mathbf{r}, t) , \tag{20a}$$

$$d(\mathbf{r}, t=0) = \delta(r - r_0)/4\pi r_0^2 , \tag{20b}$$

which is amenable to an analytical solution for the case $s(\mathbf{r}) = \delta(r - r_0)/4\pi r_0^2$ (cf. Ref. 5). A most stringent test for a numerical solution of Eq. (20) is a comparison of the recombination rate thereby predicted with its exact values. Such comparison is carried out in Table I for a sample case. Up to $t = 4$ ns the relative error is about 5%. The error on the total recombination yield at 10 ns, the quantity of interest in the calculations presented below, amounts to only 0.05%. The comparison of analytical and numerical results is, however, limited by the fact that the two calculations correspond to different forms of the optical potential $\kappa s(\mathbf{r})$.

## IV. RECOMBINATION OF THE KETYL-HEXYL RADICAL PAIR

The quantity of interest, which determines for example the magnitude of $^2\mathrm{K}\cdot$ luminescence in the experiment of Staerk and Razi Naqvi, is the yield $\phi_S$ of singlet recombination products $^1\mathrm{B} + {}^1\mathrm{RH}$ formed from the initial triplet radical pairs via the reaction route

$$^3(^2\mathrm{K}\cdot + {}^2\mathrm{R}\cdot) \xrightarrow[\text{spin motion}]{\text{diffusion}} {}^1(^2\mathrm{K}\cdot + {}^2\mathrm{R}\cdot) \xrightarrow{\text{collison}} {}^1\mathrm{B} + {}^1\mathrm{RH} .$$

In terms of Eq. (13), $\phi_S$ is

$$\phi_S = 1 - \lim_{t\to\infty} \int d\mathbf{r} [q_S(\mathbf{r}, t \mid \mathbf{r}_0, 0) + q_T(\mathbf{r}, t \mid \mathbf{r}_0, 0)] , \tag{21}$$

i.e., the fraction of radical pairs reacted. Free diffusion leads to a rapid separation of radical pairs.[5] In fact, for a diffusion constant of $10^{-5}$ cm$^2$ s$^{-1}$ the frequency of collisions between the ketyl and hexyl moieties decays to zero within a few ns. Within 10 ns after generation of the radical pairs about 90% of all re-encounters have taken place (as judged from the sample calculation for Table I). We have chosen to follow the recombination process of the ketyl–hexyl pair approximately for this length of time encompassing in our results therefore only 90% of the total singlet yield $\phi_S$. The results of our calculations are presented in Table II and III.

In our calculations we have accumulated 2000 trajectories. In order to demonstrate that this number is sufficient for the determination of the yield $\phi_S$ we add to Table II also the results of calculations which encompass 2500 trajectories in all. No significant change is observed by such extension.

Little is known about the dimensions of the spatial domain over which the hydrogen back transfer $^1(^2\mathrm{K}\cdot + {}^2\mathrm{R}\cdot) \rightarrow {}^1\mathrm{B} + {}^1\mathrm{RH}$ takes place. However, it was found that the predictions of $\phi_S$ are rather insensitive to the choice of the reaction domain. In doubling the width of the domain from 6.5–6 Å to 7–6 Å the yields increased by only about 10% (see Table II). The qualitative behavior of $\phi_S$ discussed below did not change.

TABLE I. Test of Monte Carlo approximation to Wiener's path integral.[a]

| | Recombination rate (ns$^{-1}$) | |
|---|---|---|
| Time(ns) | Analytical[b] | Monte Carlo[c] |
| 0.1 | 0.4002 | 0.3979 |
| 0.2 | 0.0994 | 0.0918 |
| 0.3 | 0.0527 | 0.0551 |
| 0.4 | 0.0366 | 0.0378 |
| 0.5 | 0.0276 | 0.0291 |
| 1.0 | 0.0112 | 0.0112 |
| 2.0 | 0.0066 | 0.0065 |
| 4.0 | 0.0020 | 0.0019 |
| 10.0 | yield = 0.08536 | yield = 0.08540 |

[a] Three-dimensional free diffusion for $r \geq 6$ Å, $D = 10^{-5}$ cm$^2$ s$^{-1}$.

[b] Assuming a $\delta$-function optical potential with $\kappa = 1.737$ Å ns$^{-1}$ corresponding to a total yield of 9.4%; rate as given by Eq. (4.13) of Ref. 5.

[c] Assuming an optical potential with $\kappa = 1.737$ ns$^{-1}$ and

$$s(r) = \begin{cases} 1/4\pi r_0^2 \text{ for } 6\ \text{Å} \leq r \leq 7\ \text{Å} \\ 0 \qquad\quad \text{for } r > 7\ \text{Å} \end{cases}$$

including 20 000 pairs in the calculation.

Table II demonstrates the typical dependence of $\phi_S$ on the applied magnetic field. In our discussion we will focus on the values corresponding to a reaction domain (6, 7 Å). At zero field 4.04% singlet products are predicted. Upon application of a field of 1 kG that value decreases to 2.30%, the reason being that the Zeeman splitting ~$gB$ of the $S_0$, $T_0$ and the $T_+$ and $T_-$ states abolishes the hyperfine-induced spin transitions from the latter. At higher fields the additional coupling ~ $\Delta gB$ between the degenerate $S_0$, $T_0$ levels develops and increases $\phi_S$ again, e.g., from a 2.30% value at 1 kG to 3.60% at 9 kG.

The results of our calculations to explore the effect of an exchange interaction acting between the radicals at contact are presented in Table III. The exchange interaction has been assumed to bring the spin motion to a halt. In our study we have considered an exchange interaction ranging from 6 to 7 Å (I) and from 6 to 8 Å (II). The predicted $\phi_S$ values for these two situations are found to be smaller than the exchange-free values (0), however, only by a marginal amount, e.g., at zero field 4.04%, 3.82%, and 3.62% for the cases (0), (I), and (II), respectively. This finding demonstrates clearly that the majority of trajectories leading to recombination are "cruising" for most of their lifetime in an area of large radical separations.

For a comparison of our results with the experiment of Staerk and Razi Naqvi we present in Fig. 3 the yield of free ketyl ions

TABLE II. Singlet recombination yield: $^3(^2\text{K}\cdot + ^2\text{R}\cdot) \rightarrow {}^1(^2\text{K}\cdot + ^2\text{R}\cdot) \rightarrow {}^1\text{B} + {}^1\text{RH}$ (in %).[a]

| Magnetic field (kG) | Recombination region 6.0–6.5 Å | Recombination region 6.0–7.0 Å |
|---|---|---|
| 0 | 3.65<br>(3.66)[b] | 4.04 |
| 1 | 2.04<br>(2.06) | 2.30 |
| 2 | 2.09<br>(2.12) | 2.37 |
| 3 | 2.19<br>(2.21) | 2.47 |
| 4 | 2.32<br>(2.34) | 2.60 |
| 5 | 2.47<br>(2.49) | 2.76 |
| 6 | 2.65<br>(2.67) | 2.95 |
| 7 | 2.85<br>(2.86) | 3.16 |
| 8 | 3.06<br>(3.07) | 3.37 |
| 9 | 3.27<br>(3.28) | 3.60 |

[a] Evaluated by a Monte Carlo calculation as described in the text averaging over 2000 diffusion trajectories; relative diffusion coefficient $D = 10^{-5}$ cm$^2$ s$^{-1}$, $r_0 = 6$ Å.

[b] Evaluated as above averaging over 2500 diffusion trajectories.

TABLE III. Singlet recombination yield: $^3(^2\text{K}\cdot + ^2\text{R}\cdot) \rightarrow {}^1(^2\text{K}\cdot + ^2R\cdot) \rightarrow {}^1\text{B} + {}^1\text{RH}$ (in %) under the influence of an exchange interaction.[a]

| Magnetic field (kG) | Exchange region 6.0–7.0 Å | Exchange region 6.0–8.0 Å |
|---|---|---|
| 0 | 3.83<br>(3.80)[b] | 3.62 |
| 1 | 2.20<br>(2.20) | 2.09 |
| 2 | 2.26<br>(2.25) | 2.14 |
| 3 | 2.35<br>(2.35) | 2.23 |
| 4 | 2.48<br>(2.49) | 2.35 |
| 5 | 2.63<br>(2.62) | 2.49 |
| 6 | 2.81<br>(2.80) | 2.66 |
| 7 | 3.00<br>(2.99) | 2.83 |
| 8 | 3.20<br>(3.18) | 3.02 |
| 9 | 3.41<br>(3.39) | 3.22 |

[a] Evaluated by a Monte Carlo calculation as described in the text averaging over 2000 diffusion trajectories; relative diffusion coefficient $D = 10^{-5}$ cm$^2$ s$^{-1}$, $r_0 = 6$ Å.

[b] Evaluated as above averaging over 2500 diffusion trajectories.

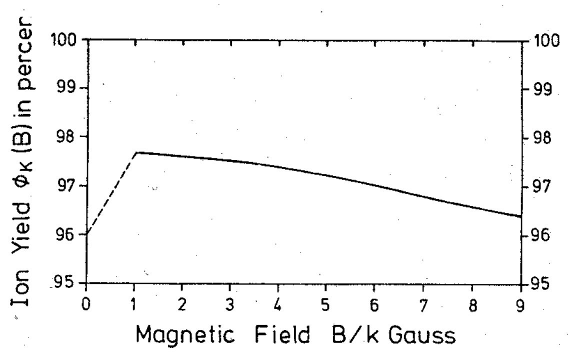

FIG. 3. Magnetic field dependence of the ketyl ion concentration at time $t = 9.5$ ns.

$$\phi_K = 1 - \phi_S , \qquad (22)$$

as a function of the magnetic field. As observed by these authors, the ketyl concentration decreases as the magnetic field increases from 1 to 9 kG. According to our calculations at zero field 96% of the ions are unreacted 9.5 ns after pair generation. This fraction increases to 97.7% at a field of 1 kG. This behavior is, however, at variance with the experimental observation[7] which established that all high field ($B > 1$ kG) ion concentration values are below the zero field values and the decrease upon varying the external field from 1 to 6 kG is over 6%.

There are several possible explanations for this discrepancy. It appears that the observed decrease of the concentration at fields $B > 1$ kG reflects a $\Delta g$ effect as described above. However, our results largely underestimate the magnitude of the decrease measured. A reason could be that the Brownian separation of the initial pair as described is too fast or the $\Delta g$-induced spin motion is too slow. The latter could be explained by a still higher $\Delta g$ value of the ketyl–hexyl radical pair than the already large value of $10^{-2}$ assumed in our calculations. The slowdown of the relative diffusion of the radicals could be due to hydrodynamic effects at short separations[17] which had been disregarded. For our calculations we have assumed, however, a rather small value for the relative microscopic diffusion coefficient of $10^{-5}$ cm$^2$ s$^{-1}$.

Another source for the discrepancy between our predictions and the observations of Ref. 7 may be due to the fact that about 50% (H. Staerk, private communication) of the fluorescing ketyl radicals observed are produced by the route $^3B^* \cdot \rightarrow {}^1B + {}^2K \cdot^*$. This reaction is also magnetic field dependent[18] and may account for a major part of the magnetic field modulation of the ketyl fluorescence. Yet another explanation may be that the formation of the ketyl–hexyl radical pair, i.e., the initial radical pair concentration is magnetic field dependent in that the field modulates either of the intersystem crossing processes $^1B^* + {}^1RH \rightarrow {}^3B^* + {}^1RH \rightarrow {}^1B + {}^1RH$. Altogether, it must be concluded that the observations of Ref. 7 escape a complete theoretical understanding, and that our analysis leaves the ketyl–hexyl pair reaction an open-ended problem.

## V. AN ANALYTICAL MODEL

It is of obvious interest to extrapolate the field behavior of the yield $\phi_S$ to higher magnetic fields. Experiments on the magnetic field modulation of radical processes in the range 10–100 kG have been carried out by Tanimoto *et al.*[20] These authors also provided an approximate theoretical analysis of the magnetic field dependence based on the Noyes step diffusion model[21] with the result that the yield of a spin-selective recombination route increases with $B^{1/2}$. Here we want to provide the exact solution of a model geminate process in which radical pairs undergoing a $\Delta g$-induced spin motion recombine to the singlet as well as to the triplet state with equal rates $\kappa$. If the pair is generated in the triplet state at $t = 0$ the probability of being in the singlet state at time $t$ at high field $B(B \gg \sum_{i,k} a_{ik})$ is

$$p_S(t) = \tfrac{1}{3} \sin^2 \omega(\mathbf{M}, B) t , \qquad (23)$$

where

$$\omega(\mathbf{M}, B) = \frac{1}{2}\left[\mu B(g_1 - g_2)/\hbar + \sum_{k=1}^{N_1} a_{1k} M_{1k} - \sum_{l=1}^{N_2} a_{2l} M_{2l}\right] , \qquad (24)$$

for the $N_1$ ($N_2$) nuclear spins of radical 1 (2), their polarization being described by the vector $\mathbf{M}$. The yield of geminate singlet recombination is given by the formal expression

$$\phi_S(\mathbf{M}, B) = \int_0^\infty p_S(t) \dot{n}(t) \, dt , \qquad (25)$$

where $\dot{n}(t)$ is the rate of reencounters defined in Ref. 5. By virtue of the results presented there

$$\phi_S(\mathbf{M}, B) = \tfrac{1}{6} \phi_\infty f\left[\kappa^2 / 2 \phi_\infty^2 D \omega(\mathbf{M}, B)\right] , \qquad (26)$$

where $\phi_\infty$ is the total recombination yield, $\kappa$ as defined in Ref. 5 and

$$f(y) = \left[1 - \sqrt{y/2}\,(1 - y)\right] / (1 + y^2) . \qquad (27)$$

The total yield is given by the sum

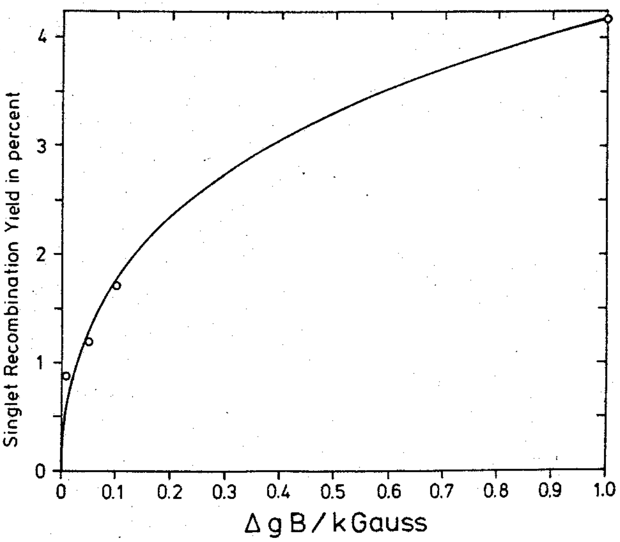

FIG. 4. Magnetic field dependence of the total singlet geminate recombination yield for a model radical process described by Eq. (30); open circles designate $\phi_S$ values for which the hyperfine coupling (3), (4) of a hexyl–ketyl pair has been taken into account.

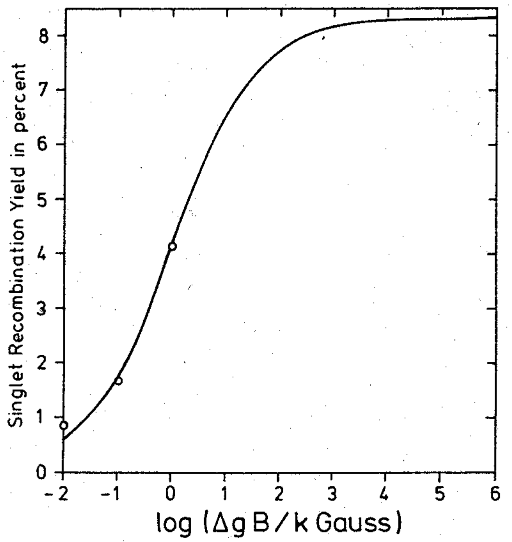

FIG. 5. Saturation behavior at very high fields of the total singlet geminate recombination yield for a model radical process described by Eq. (30); open circles designate $\phi_S$ values for which the hyperfine coupling (3), (4) of a hexyl–ketyl pair has been taken into account.

$$\phi_S(B)=2^{-N_1-N_2}\sum_{\mathrm{M}}\phi_S(\mathrm{M},B)\ , \tag{28}$$

which carries out the average over all nuclear spin orientations. In case the hyperfine interaction is negligible the result is simply

$$\phi_S(B)=\tfrac{1}{6}\phi_\infty f[\hbar\kappa^2/\phi_\infty^2 D\mu B(g_1-g_2)]\ . \tag{29}$$

For a typical situation ($D=10^{-5}$ cm$^2$ s$^{-1}$, $r_0=6$ Å, $\phi_\infty=0.5$) one has simply ($B$ in kG)

$$\phi_S(B)\approx\tfrac{1}{12}[(\Delta gB)^2-\sqrt{\Delta gB/2}+\sqrt{(\Delta gB)^3/2}\,]/[1+(\Delta gB)^2]\ . \tag{30}$$

For small $\Delta gB$ values this expression becomes proportional to $B^{1/2}$ as pointed out before.[19] The overall functional behavior of $\phi_S(B)$ given by Eq. (30) is presented in Fig. 4 for field values up to 100 kG ($\Delta g=10^{-2}$). In Fig. 5 the behavior at even higher fields is presented to demonstrate that the $\Delta g$-induced recombination saturates at extremely large magnetic field values of the order of $10^4$ kG.

## ACKNOWLEDGMENTS

The authors are grateful to Dr. Z. Schulten for her valuable suggestions and to Professor A. Weller for helpful discussions. Professor Manfred Eigen is thanked for his kind hospitality extended to I.R.E. In addition, I.R.E. thanks the National Science Foundation for a Science Faculty Professional Development Grant and the Dreyfus Foundation for a Teacher–Scholar Award. We also acknowledge the provision of computer time by the Gesellschaft für wissenschaftliche Datenverarbeitung mbH Göttingen.

[1] G. L. Closs in *Chemically Induced Magnetic Polarisation*, edited by A. R. Lepley and G. L. Closs (John Wiley, New York, 1973), pp. 117.

[2] S. K. Wong, D. A. Hutchinson, and J. K. S. Wan, J. Chem. Phys. **58**, 985 (1973).

[3] P. W. Atkins, A. J. Dobbs, G. T. Evans, K. A. McLauchlan, and P. W. Percival, Mol. Phys. **27**, 769 (1974).

[4] K. Schulten, H. Staerk, A. Weller, H.-J. Werner, and B. Nickel, Z. Phys. Chem. NF **101**, 371 (1976).

[5] Z. Schulten and K. Schulten, J. Chem. Phys. **66**, 4676 (1977).

[6] H.-J. Werner, Z. Schulten, and K. Schulten, J. Chem. Phys. **67**, 646 (1977).

[7] H. Staerk and K. Razi Naqvi, Chem. Phys. Lett. **50**, 386 (1977).

[8] (a) for an account of Wiener's work, see M. Kac, Bull. Am. Math. Soc. **72**, part II, 52 (1966); (b) a recent review on path integral methods is by F. W. Wiegel, Phys. Lett. C **16**, 58 (1975).

[9] K. Schulten and P. Wolynes, J. Chem. Phys. **68**, 3292 (1978).

[10] For a review see J. H. Freed and J. B. Pedersen, Adv. Magn. Reson. **8**, 1 (1976).

[11] P. H. Rieger and G. K. Fraenkel, J. Chem. Phys. **37**, 2811 (1962).

[12] R. W. Fessenden and R. H. Schuler, J. Chem. Phys. **39**, 2147 (1963).

[13] A misprint occurred in the corresponding Eq. (7) of Ref. 9.

[14] $\Delta g$ values fitted to the CIDNP spectra of similar reaction processes have been employed in G. L. Closs, C. E. Coubleday, and D. R. Paulson, J. Am. Chem. Soc. **92**, 2185 (1970); G. L. Closs and A. D. Trifunac, J. Am. Chem. Soc. **92**, 2186 (1970).

[15] D. L. Ermak, J. Chem. Phys. **62**, 4189 (1975); **62**, 4197 (1975).

[16] A. Farazdel and I. R. Epstein, Phys. Rev. A **16**, 518 (1977).

[17] P. G. Wolynes and J. Deutch, J. Chem. Phys. **65**, 450 (1976).

[18] K. Razi Naqvi, H. Staerk, and T. Gillbro, Chem. Phys. Lett. **49**, 160 (1977).

[19] Y. Tanimoto, H. Hayashi, S. Nagakura, H. Sakuragi, and K. Tokumaru, Chem. Phys. Lett. **41**, 267 (1976).

[20] R. M. Noyes, J. Am. Chem. Soc. **78**, 5486 (1956).